DEVELOPMENTAL BIOLOGY

Phosphorylation of Mad Controls Competition Between Wingless and BMP Signaling

Edward Eivers,*† Hadrien Demagny,* Renee H. Choi, Edward M. De Robertis‡

Bone morphogenetic proteins (BMPs) and Wnts are growth factors that provide essential patterning signals for cell proliferation and differentiation. Here, we describe a molecular mechanism by which the phosphorylation state of the *Drosophila* transcription factor Mad determines its ability to transduce either BMP or Wingless (Wg) signals. Previously, Mad was thought to function in gene transcription only when phosphorylated by BMP receptors. We found that the unphosphorylated form of Mad was required for canonical Wg signaling by interacting with the Pangolin-Armadillo transcriptional complex. Phosphorylation of the carboxyl terminus of Mad by BMP receptor directed Mad toward BMP signaling, thereby preventing Mad from functioning in the Wg pathway. The results show that Mad has distinct signal transduction roles in the BMP and Wnt pathways depending on its phosphorylation state.

INTRODUCTION

Wnts and bone morphogenetic proteins (BMPs) are crucial morphogens that instruct cells when to divide, differentiate, or die (*1*). Both signaling pathways use a distinct repertoire of molecules to carry out their specific intracellular functions. Binding of Wingless (Wg, the *Drosophila* homolog of Wnt) to its receptors causes the stabilization and nuclear accumulation of the protein Armadillo (called β-catenin in vertebrates), which forms a transcriptional complex with the DNA-binding HMG (high-mobility group) protein Pangolin [called T cell factor (Tcf) in vertebrates] (*2*). Decapentaplegic (Dpp, a BMP ligand in *Drosophila*) signals by binding to its serine-threonine kinase transmembrane receptors, causing the phosphorylation of two C-terminal serine residues in the transcription factor Mad (the *Drosophila* homolog of vertebrate Smad1). Mad then interacts with the co-Smad Medea (called Smad4 in vertebrates), accumulates in the nucleus, and activates target genes. Although both cascades can function independently of each other, an increasing number of interactions have been described between these two pathways. During development, the BMP and Wnt pathways can synergize positively (through separate binding sites in enhancer elements in the genome) (*3*, *4*), or negatively by mutual antagonism at the level of growth factor transcription (*5*–*7*). In addition, we have previously described a positive node of integration between BMP and Wnt signals at the level of phosphorylation of Mad and Smad1 (*8*, *9*).

Mad has three distinct structural domains: MH1 (Mad homology 1), which contains the DNA binding domain; MH2, which mediates protein-protein interactions; and the linker domain, which controls protein stability. Mad is phosphorylated by BMP receptors at the C terminus (Ser-Val-Ser) and by mitogen-activated protein kinase (MAPK) or cyclin-dependent kinases 8 and 9 (CDK8 and CDK9) in the linker region (*10*–*13*). These latter phosphorylation events prime for phosphorylation by glycogen synthase kinase 3 (GSK3), which triggers the polyubiquitinylation and degradation of Mad or Smad1, terminating the BMP signal (*8*, *9*). Wnt regulates this step by sequestering GSK3 inside multivesicular bodies (MVBs) (*14*), preventing GSK3-mediated phosphorylation of Mad or Smad1 and therefore prolonging the BMP signal (*15*). Here, we unexpectedly found a function for Mad in Wg signaling that is independent of phosphorylation of the C terminus of Mad. Genetic and molecular experiments show that unphosphorylated Mad binds to the Wnt transcriptional complex to activate a Wnt reporter gene, independently of its well-known role in the BMP pathway. The choice between these two distinct functions is controlled by phosphorylation, so that Mad signals in the Wg Pangolin-Armadillo pathway only when not phosphorylated by BMP receptor and GSK3.

Howard Hughes Medical Institute and Department of Biological Chemistry, University of California, Los Angeles, CA 90095–1662, USA.
*These authors contributed equally to this work.
†Present address: Department of Biological Sciences, California State University, Los Angeles, 5151 State University Drive, Los Angeles, CA 90032–8201, USA.
‡To whom correspondence should be addressed. E-mail: ederobertis@mednet.ucla.edu

RESULTS

GSK3 phosphorylation of Mad inhibits both BMP and Wg signaling

We noticed that the linker region of Mad contains more putative phosphorylation sites than previously reported (*9*), with at least 11 potential phosphorylation sites in its linker region (Fig. 1A and fig. S1A). Three are putative MAPK, CDK8, and CDK9 phosphorylation sites, which can serve as priming phosphates for a total of eight GSK3 phosphorylations (fig. S1A). Mad was stabilized by treating *Drosophila* S2R+ cells with Wg-conditioned medium (fig. S1, B and C). In addition, a form of Mad in which all eight GSK3 phosphorylation sites in the linker region were mutated into alanines (referred to as Mad-GM8) was no longer stabilized by Wg (fig. S1, B and C), indicating that the stabilization of Mad by Wg requires intact GSK3 phosphorylation sites in its linker region. As expected for a transcription factor involved in the BMP pathway (*8*, *9*), the stabilized Mad mutant (Mad-GM8) increased the activity of a BMP reporter gene containing a BMP response element driving luciferase expression (Fig. 1B and fig. S1D), and inhibition of GSK3 by lithium chloride (LiCl) prolonged the duration of BMP signaling after a short BMP pulse (fig. S1E). In the wing imaginal disc, Brinker acts as a transcriptional repressor of genes activated by Dpp, and one of the functions of Dpp-activated Mad is to inhibit *Brinker* transcription (*16*). In vivo, expression of stabilized Mad (Mad-GM8) increased BMP signaling in wing imaginal discs as demonstrated by reduced expression of *Brinker* (Fig. 1, C to E). Mad-GM8 also induced ectopic wing vein formation, a phenotype typical of excess BMP signaling, to a greater extent than caused by the previously described form of Mad with mutations in two GSK3 sites (Mad-GM2) (*9*) (fig. S1,

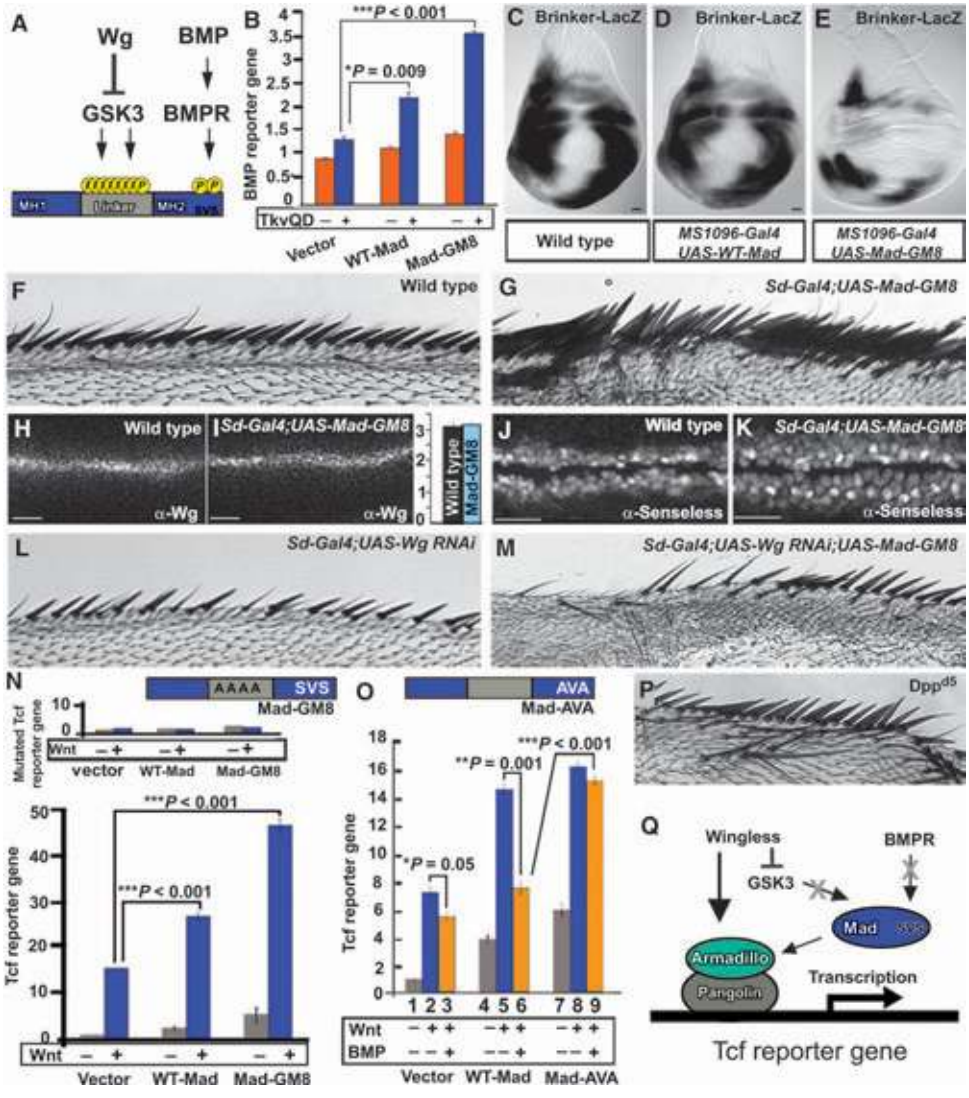

Fig. 1. The phosphorylation state of Mad determines whether it signals through the BMP or the Wg pathway. (**A**) GSK3 and BMP receptor (BMPR) phosphorylation sites in Mad. (**B**) Wild-type Mad (WT-Mad) and Mad-GM8 increased the activity of the BMP reporter gene [$*P = 0.009$; $***P = 0.001$, two-way analysis of variance (ANOVA) with Tukey's post test]. The BMP pathway was stimulated with an activated BMP receptor, activated Thickveins (TkvQD), in *Drosophila* S2 cells. (**C** to **E**) Mad-GM8 increased BMP signaling as indicated by repressed *Brinker* expression in wing discs. $n = 16$ (C), $n = 8$ (D), and $n = 7$ (E). (**F** and **G**) WT ($n = 31$) and ectopic wing margin bristles induced by Mad-GM8 overexpression ($n = 40$). (**H** to **K**) Mad-GM8 did not alter endogenous Wg amounts ($P > 0.66$, $n = 20$ intensity measurements) but did increase the area of the Wnt target Senseless ($P = 0.0086$, $n = 20$ intensity measurements; Mann-Whitney Wilcoxon test). Numbers of wing discs examined were $n = 40$ (H), $n = 10$ (I), $n = 16$ (J), and $n = 12$ (K). (**L** and **M**) Sensory bristle induction by Mad-GM8 required endogenous Wg. $n = 16$ (L) and $n = 17$ (M). (**N**) WT-Mad and Mad-GM8 increased Tcf reporter gene activity in HEK293T cells, effects that were abolished by mutating the Tcf DNA binding sites (inset) ($***P < 0.001$, two-way ANOVA with Tukey's post test; $n = 6$ experiments). (**O**) Tcf reporter gene induction by WT-Mad, but not by phosphorylation-resistant Mad-AVA, is repressed by treating cells with BMP4 ($*P = 0.05$; $**P = 0.001$; $***P < 0.001$, two-way ANOVA with Tukey's post test; $n = 3$ independent experiments). (**P**) Ectopic bristles in Dpp^{d5} (*24*) mutant wings ($n = 12$, 7 wings with extra bristles). (**Q**) Proposed model in which Mad interacts with the Wg transcriptional complex. Scale bars, 20 μm.

F to O). We conclude that GSK3 phosphorylation regulates the duration of the BMP signal through Mad (*8*, *9*).

In addition to the phenotypes noted above indicative of high BMP signaling, the stabilized form of Mad (Mad-GM8) caused induction of sensory bristles along the margin of the wing (Fig. 1, F and G). This phenotype is typically associated with increased Wg signaling (*17*), prompting us to investigate the molecular mechanism by which Mad functions in the Wg pathway. The induction of bristles by stabilized Mad took place without changes in Wg protein abundance (Fig. 1, H and I). However, the area of Wg targets such as Senseless (Fig. 1, J and K) and Distalless (fig. S2) was expanded by expression of Mad-GM8. This bristle induction required endogenous Wg (Fig. 1, G, L, and M, and fig. S3). Furthermore, Mad-GM8 overexpression induced phenotypes in eye imaginal discs reminiscent of those caused by gain-of-function mutations for Wg, such as transdetermination of adult eye cells into antenna-like tissue (fig. S4) (*18*, *19*).

We next investigated whether Mad could activate a Tcf reporter gene (Super 7x TOPFLASH luciferase). Tcf reporter activity after Wnt3a treatment was increased by expression of wild-type Mad and to a greater extent by expression of stabilized Mad-GM8 (Fig. 1N). As a control, we used a mutated Tcf reporter gene (Super 7x FOPFLASH luciferase) that cannot bind Tcf, and, as expected, this reporter gene failed to respond to wild-type or stabilized Mad transfection (inset in Fig. 1N), demonstrating that Mad requires Tcf binding sites to activate Wnt signaling. Together, these data indicated that inhibition of the GSK3-mediated phosphorylations of Mad enhances cellular responsiveness not only to BMP but also to Wnt.

Mad activates Wg target genes independently of phosphorylation of its C terminus

To rule out the possibility that Mad caused ectopic margin bristles by increasing BMP signals, we carried out three experiments. First, Dpp misexpression in wing discs caused loss of margin bristles (fig. S1J). Second, addition of BMP4 inhibited stimulation of Wnt signaling in cells transfected with empty vector (Fig. 1O); inhibition by BMP4 was more marked in cells transfected with wild-type Mad (Fig. 1O). Third, a mutant with a partial Dpp loss of function (Dpp^{d5}) (*20*) developed ectopic anterior

margin bristles (Fig. 1P), a phenotype indicative of increased Wg signaling. We conclude from these results that Dpp signaling normally inhibits canonical Wg signaling and that Mad may therefore induce Wg signaling through a Dpp-independent pathway.

To investigate this BMP-independent function further, we constructed a C-terminal phosphorylation-resistant mutant Mad by mutating the serine residues phosphorylated by BMP receptor (Ser-Val-Ser) into alanine residues (Ala-Val-Ala) (Mad-AVA) (Fig. 1O). This mutant form of Mad was inactive in the BMP pathway when compared to wild-type Mad (fig. S1D), but activated Tcf reporter gene assays (Fig. 1O, bar 8). In addition, the effect of Mad-AVA expression on Tcf reporter gene activity was no longer inhibited by BMP addition (Fig. 1O, bars 6 and 9, and fig. S5). These results suggested a molecular mechanism by which Mad interacts with the Wnt transcriptional complex in the absence of active BMP signaling (Fig. 1Q).

To demonstrate that nonphosphorylated Mad functions in Wg signaling in *Drosophila*, we tested two C-terminal mutant forms of Mad, Mad^{10} (*21*) and Mad^{12} (*22*), which lack C-terminal but retain linker phosphorylation sites (Fig. 2A) (*9*). *Drosophila* S2R+ cells transfected with phosphorylation-resistant Mad-AVA, Mad^{10}, or Mad^{12} showed increased Tcf reporter gene activity in response to Wg (Fig. 2, B and C). In wing discs, Mad^{12} clones showed ectopic distribution of Distalless (arrows) close to sources of Wg protein production (Fig. 2, D to J). Distalless is a specific reporter for Wg signaling in the wing disc (*23*). Mad^{10} clones can also induce ectopic distribution of Distalless in wing imaginal discs (*24*). However, Mad^{12} clones distant from Wg sources failed to induce ectopic production of Distalless (Fig. 2H, arrowheads), suggesting that the induction of Wg signaling by Mad requires additional components, such as stabilized Armadillo, which is only found close to sources of Wg. These data demonstrate that the function of Mad in Wnt signaling occurs independently of BMP-induced phosphorylation of the C terminus of Mad. Increased abundance of the Wg target Distalless in Mad^{12} mutant clones (Fig. 2I) indicates that phosphorylation of the C terminus of Mad normally inhibits Wnt signaling at endogenous amounts of this transcription factor in vivo.

Mad and Medea are required for Wg signal transduction

We next examined the requirement of full-length Mad in Wg signal transduction. Because deletion alleles of Mad are not available, we used Mad RNA interference (RNAi) clones (*9*). Wing discs with Mad RNAi clones lacked Distalless (Fig. 3, A to D), whereas endogenous Wg was unaffected (Fig. 3, E and F). The phenotype caused by this Mad RNAi was specific because it was rescued in the whole adult wing with a UAS-Smad1 transgene expressing the human homolog of Mad (fig. S6). Mad knockdown throughout the developing wing pouch reduced the abundance of Wnt target Senseless (Fig. 3, G and H) and prevented Dishevelled overexpression from inducing ectopic Senseless in the wing pouch (Fig. 3, compare I to J, and fig. S7, A to D). This epistatic experiment showed that Mad is required downstream of Dishevelled in the Wnt pathway. Similarly, formation of increased numbers of sensory bristles by Dishevelled overexpression was inhibited by Mad RNAi (fig. S7, E to L). Furthermore, Tcf reporter gene activity in S2R+ cells was reduced by Mad RNAi (Fig. 3K), an inhibitory effect that was rescued by overexpression of human Smad1 (fig. S7M).

In addition, we found a requirement for Armadillo (*25*) and Medea in Wg signaling in *Drosophila* S2R+ cells and for Smad4 and β-catenin in human embryonic kidney (HEK) 293T cells (Fig. 3, L and M, and fig. S7, N to P). These observations are consistent with previous reports that Smad4 interacts with β-catenin in the activation of *Xenopus* homeobox genes (*26*, *27*). We conclude that Mad and Medea are required for Wg signaling, both in Tcf reporter assays of Wg activity and in vivo in *Drosophila*.

Mad binds to Pangolin in the absence of phosphorylation of its C terminus

Next, we examined whether Mad could bind to the Pangolin-Armadillo complex.

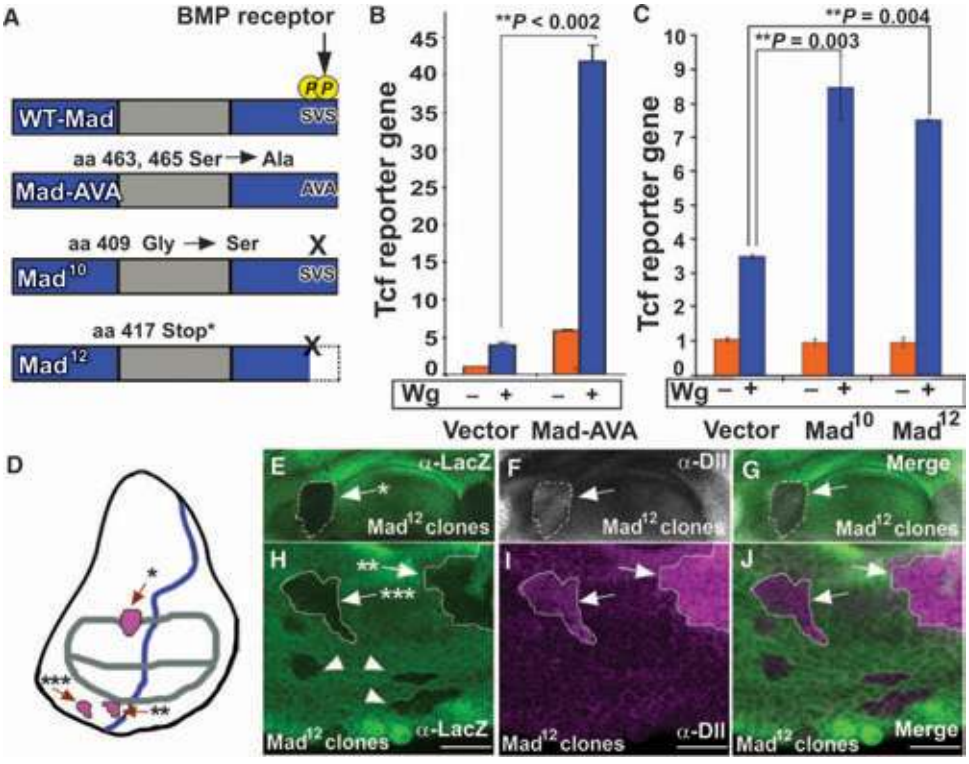

Fig. 2. Mad transduces Wg signals independently of BMP activity. (A) Diagrams of WT-Mad and phosphorylation-resistant C-terminal Mad mutant proteins. (B and C) Mad C-terminal phosphorylation-resistant mutants increase Wg signaling, as measured by Tcf reporter gene activity in *Drosophila* S2R+ cells (**P = 0.002; **P = 0.004; **P = 0.003, two-way ANOVA with Tukey's post test; n = 3 experiments). (D) Diagram of third instar wing imaginal disc with the location of clones shown indicated by arrows and asterisks; regions of Wg (gray) and Dpp (blue) sources are outlined. (E to J) Mitotic Mad^{12} clones in the wing imaginal disc activate the downstream Wg target Distalless near Wg sources. Clones distant to sources of Wg do not activate Distalless and are indicated by arrowheads. This induction of the Wg target occurred at endogenous amounts of Mad (n = 15 clones from seven wing discs with ectopic Distalless). Scale bars, 20 μm.

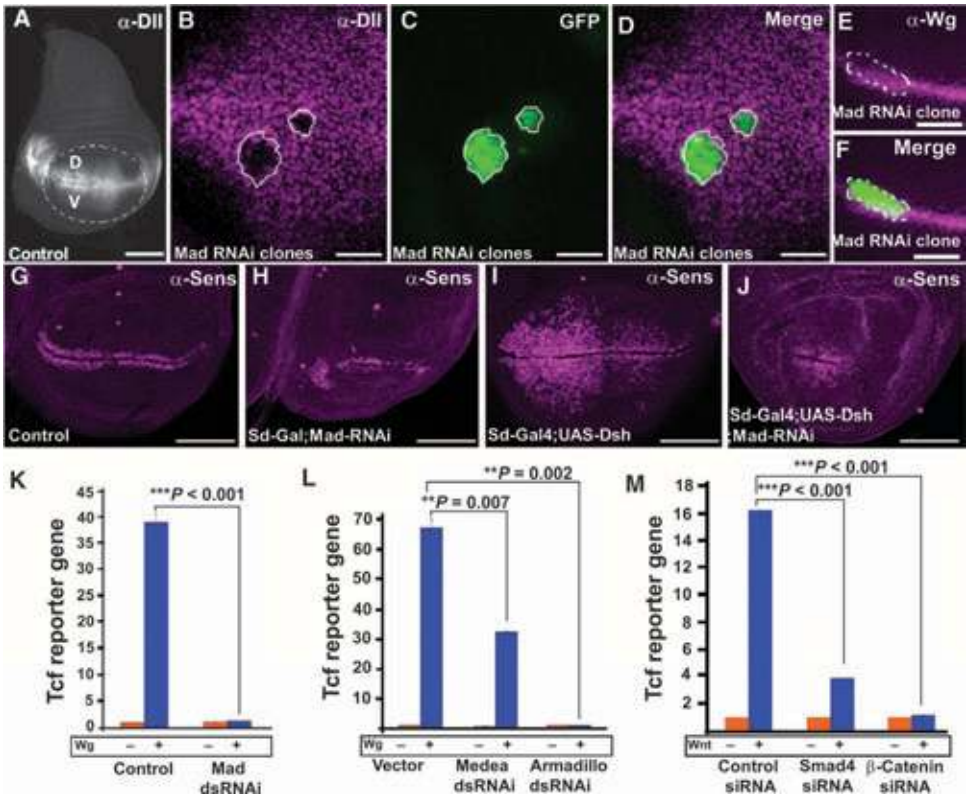

Fig. 3. Mad and Medea are required for Wg signal transduction. (**A**) Wild-type distribution of Distalless in a wing imaginal disc. Scale bar, 100 μm. (**B** to **D**) Decreased abundance of the Wnt target Distalless in Mad RNAi clones in the ventral (V) wing pouch. *n* = 10 clones in the region where Distalless is normally found, all showing decreased Distalless abundance. Scale bar, 20 μm. (**E** and **F**) Wg production was maintained in Mad RNAi clones (*n* = 14 clones; scale bar, 50 μm). (**G** to **J**) The area of Senseless in wing imaginal discs was reduced in clones expressing Mad RNAi or those expressing both UAS-Mad RNAi and UAS-Dishevelled. At least 12 discs per genotype were analyzed, with similar results. Scale bars, 100 μm. (**K**) Knockdown of Mad by dsRNA inhibited the activity of the Tcf reporter gene in *Drosophila* S2R+ cells (***P < 0.001, two-way ANOVA with Tukey's post test, *n* = 6 experiments). (**L**) Knockdown of Medea or Armadillo by dsRNA blocked Wg signaling in S2R+ cells (**P = 0.007; **P = 0.002, two-way ANOVA with Tukey's post test, *n* = 3 experiments). (**M**) siRNAs against Smad4 or β-catenin inhibited Wnt reporter responses in HEK293T cells (***P < 0.001, two-way ANOVA with Tukey's post test, *n* = 3 experiments).

A previous report had described that the mammalian Mad homolog Smad1 interacted with β-catenin and Tcf to activate *Myc* transcription (*28*). Mad-Flag, Armadillo–HA (hemagglutinin), and Pangolin-Myc were transfected separately into HEK293T cells and cell lysates were prepared. To stabilize Mad and Armadillo, we treated all cultures with the GSK3 inhibitor 6-bromoindirubin-3′-oxime (BIO) (*29*). We later found that preventing GSK3 phosphorylation of Mad increased binding efficiency (fig. S8, A and B). Less Mad bound to Pangolin in lysates from transfected cells treated with a pharmacologically inactive form of BIO, 1-methyl BIO (*29*) (fig. S8C).

Mad and Armadillo failed to bind to each other (Fig. 4A). However, in the presence of Pangolin, Mad-Flag pulled down Pangolin and Armadillo (Fig. 4B). Thus, Pangolin mediates the binding of both Mad and Armadillo. Moreover, Mad-AVA bound Pangolin to a similar extent as wild-type Mad (Fig. 4B, compare lanes 2 and 3), suggesting that phosphorylation of the C terminus of Mad is not required for binding of Pangolin. Binding of Mad to Pangolin was previously reported, but it was suggested that the binding of Mad inhibited the interaction between Armadillo and Pangolin (*24*). The different findings might be due to our use of a GSK3 inhibitor, which stabilizes Mad and Armadillo. As described previously, Mad^{10} mitotic clones show increased abundance of the Wg target Distalless in wing discs (*24*). Therefore, we propose that because Mad^{10} or Mad^{12} cannot be phosphorylated by BMP receptors, more Mad protein is available to signal through the Wg pathway. We conclude from these biochemical experiments that Mad, Pangolin, and Armadillo can form protein complexes in cell extracts, independently of the phosphorylation of the C terminus of Mad.

Next, we asked whether binding of Mad to Pangolin was inhibited by phosphorylation of its C terminus. We cotransfected HEK293T cells with Mad-Flag and Pangolin-Myc, with or without a constitutively active Alk3 BMP receptor (CA-Alk3). As expected, expression of CA-Alk3 resulted in phosphorylation of the two C-terminal serine residues of Mad (Fig. 4C, compare lanes 5 and 6). Pangolin-Myc immunoprecipitated Mad-Flag only in cells lacking the constitutively active Alk3 receptor (Fig. 4C, compare lanes 2 and 3). Activation of BMP signaling with expression of the constitutively active Alk3 receptor significantly reduced binding of Mad to Pangolin. These experiments indicate that the phosphorylation of the C terminus of Mad has an inhibitory effect on the formation of complexes with Pangolin.

The Pangolin-Mad-Armadillo complex binds to Tcf DNA binding sites

Using a DNA affinity precipitation assay (*30*), we asked whether the protein complex of Pangolin and Mad could interact with Tcf DNA binding sites. A 5′ biotin-labeled and a 3′ unlabeled primer were used to amplify by polymerase chain reaction (PCR) the seven Tcf binding repeats (table S1) of the Tcf reporter gene (SuperTOPFLASH) or its mutated counterpart (SuperFOPFLASH), in which all seven specific binding sites for Tcf are mutated. Biotin-labeled PCR products were then bound to streptavidin-agarose beads and lysates from Wg-treated *Drosophila* S2R+ cells transfected with Mad-Flag were incubated with streptavidin-biotin-DNA beads. We found that Mad-Flag and two isoforms of endogenous Pangolin bound to Tcf reporter gene DNA (Fig. 4D, lane 2). Mad binding to the mutated Tcf reporter gene product was barely detectable (Fig. 4D, lane 1). In addition, extracts containing C-terminally phosphorylated Mad displayed decreased association with DNA containing Tcf binding sites (Fig. 4E). In conclusion, these biochemical experiments suggest that Mad preferentially binds to the Pangolin-Armadillo complex on Tcf binding sites in DNA in the absence of phosphorylation of the C terminus by BMP receptor. The results uncover a role for nonphosphorylated Mad in Wg signaling transduction.

DISCUSSION

We investigated how the phosphorylation state of the transcription factor Mad can determine its ability to transduce a BMP or a Wnt signal in the cell. The molecular mechanism depicted in Fig. 5 proposes a new layer of regulation in canonical Wg signaling. Mad is required for Wg signaling both in Tcf reporter gene assays and in vivo in *Drosophila*. This aspect of Mad activity is inhibited by phosphorylation by BMP receptor resulting from activation of the BMP pathway. Wnt signaling sequesters GSK3 from the cytosol into MVBs (*14*), causing stabilization of Armadillo and Mad, which then binds to Pangolin. This protein complex can bind to Tcf binding sites in DNA to control the transcription of Wnt target genes. The proteins encoded by the *Drosophila* Mad[10] and Mad[12] genetic mutants have lost the BMP receptor branch of their function, but retain their ability to engage in Wg signaling (Fig. 2). Interactions between Dpp and Wg signaling, both positive (*3*, *4*) and negative (*5*–*7*), have been reported in *Drosophila*. We propose that the BMP pathway would have positive interactions with Wg only for genes with both BMP and Wg response elements in their promoters (*3*, *4*). In most other cases, we suggest that the BMP and Wg pathways compete for the available pool of Mad (Fig. 5).

Our findings suggest that Dpp signaling can generate an inverse gradient of Wnt activity because high BMP activity competes for Mad and Medea, reducing their availability to signal in the Wg pathway. Unphosphorylated Mad can participate in Wg signaling when only Pangolin binding sites are present in an enhancer. When BMP receptor phosphorylates Mad, a trimer with Medea would be formed that would direct Mad to BMP responsive promoters (Fig. 5). It has been proposed that Smad4 is the limiting component in cells transducing BMP and transforming growth factor–β (TGF-β) signals (*31*). In a cell receiving both BMP and Wnt signals, Mad phosphorylated at the C terminus would compete with unphosphorylated Mad for limited amounts of Medea. Moreover, most cellular Smad1 has been reported to enter the nucleus in response to BMP2 treatment (*32*), suggesting that the competition between BMP and Wnt signaling could occur directly at the level of Mad as well.

This study advances our understanding of signaling crosstalk between the Wg and the BMP pathways in several ways. First, it shows that Mad, a transcription factor classically associated with the BMP pathway, is also an effector of canonical Wnt signaling. Second, BMP receptor–mediated phosphorylation of Mad is not required for activity in the Wnt pathway. Instead, mutations such as Mad[12] that truncate the C terminus increase Wnt signaling at endogenous protein amounts. Third, phosphorylation of the linker region of Mad by GSK3 has an inhibitory

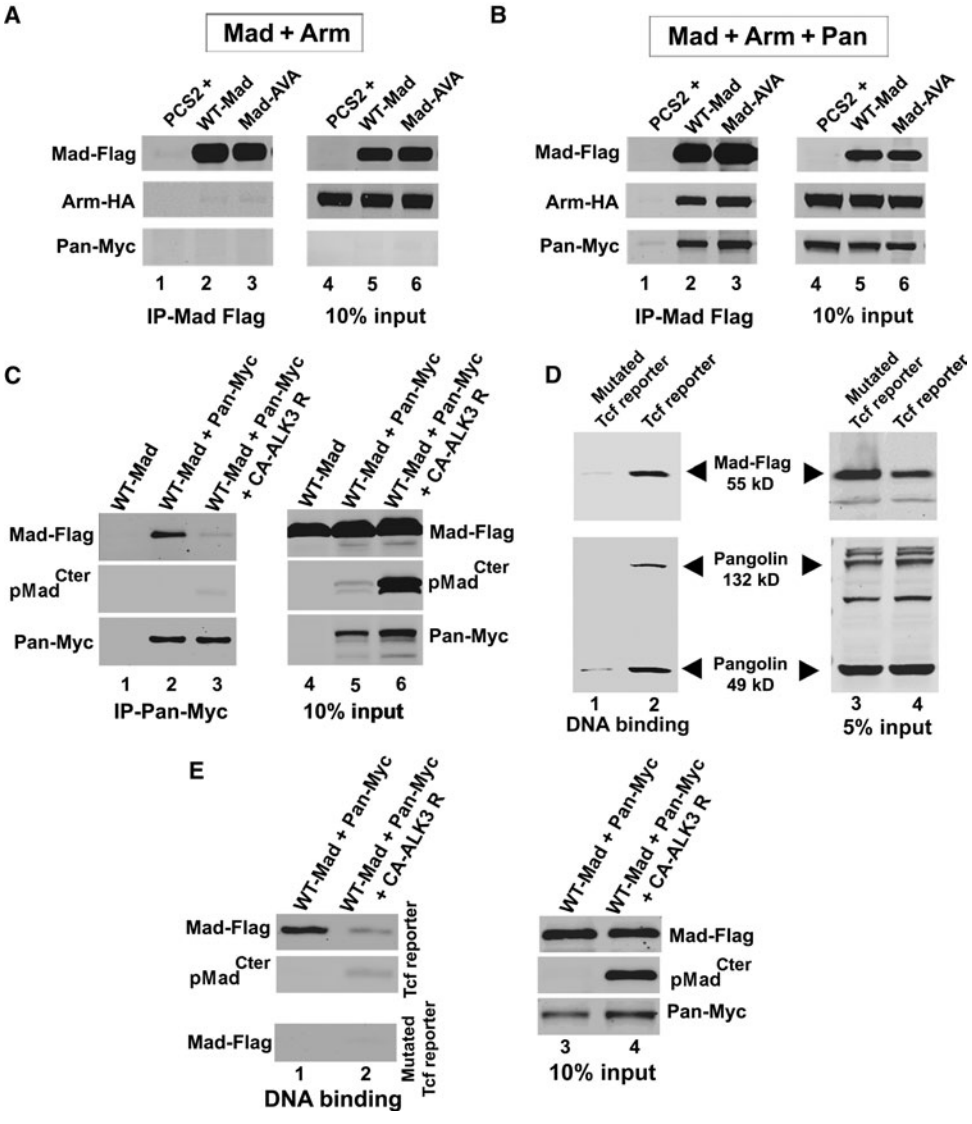

Fig. 4. Mad is a component of the Wnt transcriptional complex bound to DNA. (**A**) Mad-Flag did not immunoprecipitate with Armadillo in the absence of Pangolin (n = 4 experiments). (**B**) Mad-Flag bound Pangolin, which also coimmunoprecipitated with Armadillo (n = 3 independent experiments). (**C**) Pangolin-Myc immunoprecipitated unphosphorylated Mad-Flag (lane 2). Less Mad-Flag bound to Pangolin-Myc (lane 3) in cells expressing a constitutively activated BMP receptor (CA-ALK3 receptor) (which would be expected to trigger phosphorylation of sites in the C-terminal domain). Binding of Mad to Pangolin was significantly reduced (P = 0.0014, t test; n = 3 independent experiments). (**D**) Biotin-labeled PCR products containing Tcf binding sites bound both Pangolin and Mad-Flag proteins (lane 2) from S2R+ cell lysates in a DNA affinity precipitation assay. Pangolin was detected by immunoblotting. PCR products containing mutated Tcf binding sites failed to bind Pangolin or Mad proteins (lane 1) (n = 3 experiments). (**E**) Pangolin-Myc and Mad-Flag bound to PCR products containing Tcf binding sites (lane 1, top panel) but not to those containing mutated Tcf binding fragments (lane 1, bottom panel). C-terminally phosphorylated Mad-Flag extracts did not bind to the PCR products containing Tcf binding sites (lane 2, top panel). Inputs are shown in lanes 3 and 4.

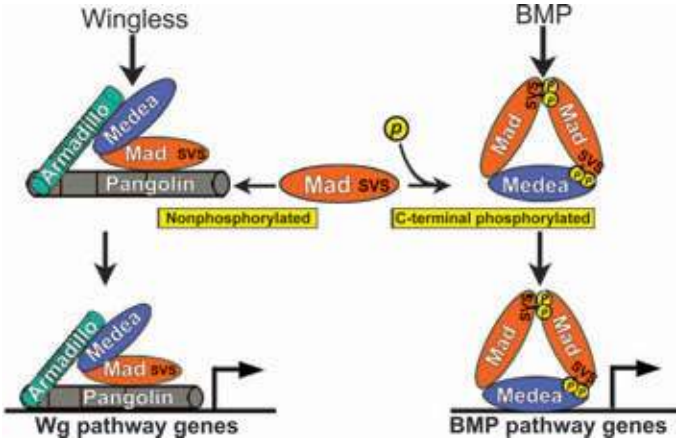

Fig. 5. Proposed model in which Mad and Medea bind to the Wg Pangolin-Armadillo transcriptional complex in the absence of BMP signals. Previously, Mad was believed to be transcriptionally active only when phosphorylated at its C terminus by BMP receptor. In this model, Mad promotes activation of Wg pathway target genes when not phosphorylated. In the presence of BMP, Wg serves to prolong the signal from Mad phosphorylated in the C-terminal domain by inhibiting GSK3-mediated phosphorylation of the linker region of Mad (*8*, *9*). In addition, BMP signaling also diverts Mad or Medea from the Wg pathway to promote activation of BMP target genes, thereby causing competition between the BMP and the Wingless pathway.

effect on Wnt signaling. This previously unknown phosphorylation-independent function of Mad has implications for cell differentiation and cancer.

MATERIALS AND METHODS

Drosophila stocks

Drosophila strains used in this work were as follows: *UAS-WT-Mad*, *UAS-Mad-GM8/Cyo*, *UAS-Mad-GM2*, *UAS-human-Smad1*, *UAS-Dishevelled* (#9453), *UAS-DN-GSK3*, *UAS-ArmS10* (#4782), *hsflp;UAS-Mad RNAi;UAS-Mad-RNAi*, *UAS-Wg-RNAi* (Vienna *Drosophila* RNAi Center, VDRC #13352). Gal4 drivers used (Bloomington stock number in parentheses) were as follows: *MS1096-Gal4*, *Scalloped-Gal4* (#8609), *Engrailed-Gal4* (#6356), *Eyeless-Gal4*, and *yw;Act>y*$^{+}$*>Gal4;UAS-GFP*. Other strains used in this study were *Brinker-LacZ*, *Dpp[d5]/Cyo* (#2071), and *Canton S*.

Clonal analysis

For random heat shock "flip-out" clones, we crossed females of the genotype *yw;Act>y*$^{+}$*>Gal4;UAS-GFP* to males of the genotype *ywhsflp;Mad-RNAi/Mad-RNAi*. Flies laid eggs for 6 to 8 hours, and eggs were incubated for a further 16 to 20 hours at 25°C. Larvae at first instar were administered single heat shocks (37°C) ranging from 5 to 15 min. An RNAi approach was used because no complete loss-of-function Mad mutants exist at present; the most precisely defined deletion of Mad Df(2L)C28 removes a number of other genes (*33*). The Mad RNAi construct used previously described Mad sequences (*9*) placed in a Gal4-inducible pWiz vector (*34*). Mitotic *Mad*^{12} clones were induced by crossing female *ywhsflp;Arm-LacZM21FRT40/Cyo-GFP* with *ywhsflp;Mad12FRT40/Cyo* males. Flies laid eggs for 8 hours, and eggs were incubated for a further 16 to 28 hours at 25°C. Larvae at the first instar were administered single heat shocks (37°C) ranging from 20 to 30 min. After heat shock, larvae were grown at 25°C for recovery and further development.

Mounting of adult wings

Wings were removed from adult flies and dehydrated in 100% ethanol for 5 min. The wings were placed on a slide with the dorsal side up, and the ethanol was allowed to evaporate. A small drop of Canada balsam was dropped onto the wing and a glass coverslip was placed on top. A 10-g weight was used to flatten the preparation.

Wing disc fixation and immunostaining

Wing discs were dissected from third instar larvae in cold 0.02% Triton X-100 phosphate-buffered saline (PBS) (PBST) solution. Discs were fixed in 4% formaldehyde for 20 min on ice and rinsed with PBST. Discs were then incubated in blocking solution (2.5% bovine serum albumin and 5% goat serum in PBS/0.02% Triton X-100) for 1 to 2 hours at room temperature. Primary antibodies—α-Senseless (1:10; gift of H. Bellen), α-Distalless (1:300; gift of I. Duncan) (*35*), α-LacZ (1:1000), or α-Wg (1:200; Developmental Hybridoma Bank)—were incubated in blocking solution overnight at 4°C and washed 10 times for 2 hours in PBST. Discs were incubated for 1 to 2 hours in blocking solution and incubated for 1 hour in anti-mouse Cy3-conjugated secondary antibody (1:1000, Jackson Laboratory) at room temperature. Wing discs were placed in DAPI (4′,6-diamidino-2-phenylindole)–containing Vectashield (Vector) overnight and mounted on glass slides.

Reporter gene assays in *Drosophila* S2 and HEK293T cells

To test whether stabilized Mad linker mutants could activate a BMP reporter gene (BRE-luciferase) (*36*) to a greater extent than wild-type Mad, we cotransfected pAC-Mad (0.1 μg), BMP reporter gene (0.1 μg), and thymidine kinase (TK)–*Renilla* (0.01 μg) constructs with an activated form of the Thickveins receptor (pAC-TKVQD, 0.1 μg) (*37*) into S2 cells. Luciferase readings were measured 48 hours after transfection with the Promega Dual-Luciferase Reporter Assay System. S2 cells produce the BMP ligands Dpp and Glass bottom boat (Gbb), and pMad^{Cter} is readily detected in nuclei. For this reason, we also used HEK293T cells, which have no detectable amounts of pSmad1^{Cter}, to carry out Wnt reporter assays. HEK293 cells were cultured in 12-well plates and transiently transfected with Fugene (Roche). *Renilla* luciferase pRLCMV served as the internal control. Transfections contained 0.2 μg of SuperTOPFLASH Tcf reporter gene (*38*), 0.02 μg of pRL-CMV, and 0.5 μg of the various pCS2-Mad constructs. pCMV empty vector was used to reach a total of 0.72 μg of DNA per well. Wg-conditioned medium from permanently transfected S2 cells (*Drosophila* Genomics Resource Center, stock #165; originally from R. Nusse) was used to treat *Drosophila* S2R+ cells. For 293T cells, Wnt3a-conditioned medium from permanently transfected L cells (gift of R. Nusse) was used.

Luciferase assays were performed with the Dual-Luciferase Reporter Assay System (Promega) according to the manufacturer's instructions, and the results were standardized against internal *Renilla* controls. To assess the duration of BMP signals (fig. S1E), we transfected cells with BMP reporter gene (BRE-luciferase) (*36*) with wild-type Mad in a six-well plate. Twelve hours later, cells were starved in serum-free medium for 4 hours, and 5 nM BMP7 (R&D Systems) was added for 30 min. Cells were washed in serum-free medium and incubated with or without 30 mM LiCl to inhibit GSK3.

Gene silencing in *Drosophila* S2R+ cells and HEK293T cells

Double-stranded RNA was used to knock down Mad, Medea, and Armadillo in S2R+ cells. RNA design and treatment was based on the protocol

by Clemens and co-workers (*39*). Primer sequences are found in table S1. The Ambion MEGAscript kit was used for double-stranded RNA (dsRNA) amplification. Cells were treated with Mad, Medea, or Armadillo dsRNA for 4 days. Cells were transfected on day 3 with Tcf reporter gene (0.4 μg) (*38*) and pTK-*Renilla* (0.04 μg) with Effectene (Qiagen). On day 4, cells were treated with Wg-conditioned medium or control medium for 8 hours.

To rescue Mad knockdown in S2R+ cells, we used a human Smad1 construct (in pAC 5.1 vector) transfected together with a copper-inducible pWiz-Mad RNAi construct (*34*). Transfection of pWiz-Mad RNAi (0.1 μg), metallothionein-Gal4 (0.1 μg), SuperTOPFLASH luciferase (0.1 μg), and pTK-*Renilla* (0.01 μg) was carried out with Qiagen Effectene. S2R+ cells were grown for a total of 4 days and then treated with either Wg-conditioned medium or control medium for 8 hours.

For small interfering RNAs (siRNAs) in HEK293T cells, siRNAs targeting human β-catenin and Smad4 were ON-TARGETplus SMARTpool from Thermo Scientific (#L-003482 and #L-003902, respectively). Control siRNA was BLOCK-iT Fluorescent Oligo (Invitrogen, #44-2926). siRNAs were transfected with Lipofectamine 2000 by means of the reverse transfection protocol (Invitrogen) and analyzed after 48 hours. Cells were first transfected with siRNA and then with DNA 24 hours later.

Coimmunoprecipitation assays

HEK293T cells were cultured in six-well plates and transiently transfected with DNA using Fugene (Roche). pCMV-Pangolin-Myc, pCS2-Mad-Flag, and pCMV Armadillo-HA plasmid DNAs were transfected separately into HEK293T cells and treated with 5 μM GSK3 inhibitor BIO for 4 hours (*27*). The use of BIO in this experiment was essential to ensure efficient binding, because GSK3 phosphorylations inhibit complex formation (fig. S8). The Pangolin and Armadillo constructs were gifts of E. Verheyen (*24*). Cells were lysed with a standard lysis buffer [50 mM tris (pH 7.4), 150 mM NaCl, 1 mM EDTA, and 1% Triton X-100]. Usually, 250 μl of cell lysate containing Mad proteins was incubated with 250 μl of lysates containing tagged proteins at 4°C with end-over-end rotation for 1 hour. For the binding of Mad-Flag, Armadillo-HA, and Pangolin-Myc, 166 μl of each lysate was added. Immunoprecipitation of Mad-Flag was carried out with anti-Flag beads (Sigma). Beads were centrifuged at 1000*g* for 1 min. The bound proteins were washed three times with 1 ml of tris-buffered saline (TBS) and then eluted with 200 μl of TBS containing FLAG peptide (100 μg/ml; Sigma) with end-over-end rotation for 30 min at 4°C. The results were analyzed by Western blot. The antibodies used were anti-Flag mouse (Sigma), 1:1000; anti–c-Myc mouse (Santa Cruz), 1:1000; anti-Smad1^{Cter}, 1:1000 (*40*); and anti-HA (Sigma), 1:1000. Pangolin-Myc, Mad-Flag, and CA-ALK3 receptor were cotransfected into HEK293T cells for experiments testing whether C-terminally phosphorylated Mad bound Pangolin. Cells transfected with or without CA-ALK3 were treated with the GSK3 inhibitor BIO for 6 hours before lysate preparation. Pangolin-Myc immunoprecipitation was carried out with anti-Myc beads (Covance AFC-150P) under conditions in which Mad was phosphorylated or not. Elution was performed with Myc peptide (100 μg/ml; Sigma).

DNA affinity precipitation assay

The sequence encoding the seven Tcf binding sites present in the SuperTOPFLASH luciferase reporter (Tcf reporter gene) plasmid was amplified by PCR (*38*). The primers used were a forward biotin-labeled primer and a nonbiotinylated 3′ reverse primer (table S1). As a negative control, the same primers were used to amplify the sequence of the SuperFOPFLASH luciferase reporter (mutated Tcf reporter gene) (*38*). The biotinylated PCR products were incubated for 1 hour at 4°C with streptavidin-agarose beads (Sigma, S1638-5ML) (*30*). The beads were then washed three times with binding buffer [10% glycerol, 4 mM tris-Cl (pH 7.9), and 60 mM KCl] to remove unbound PCR products. DNA-biotin-avidin agarose beads were then added to S2R+ cell extracts overexpressing wild-type Mad-Flag. Transfected S2R+ cells were lysed with a modified lysis buffer: 10% glycerol, 4 mM tris-HCl (pH 7.9), 60 mM KCl, and 1% Triton X-100. Cell lysates and beads were incubated overnight at 4°C with end-over-end rotation to allow proteins to bind to DNA (*30*). The beads were then centrifuged at 1000*g* for 1 min. Bound proteins were washed three times with 1.5 ml of binding buffer [10% glycerol, 4 mM tris-HCl (pH 7.9), and 60 mM KCl] and then eluted by adding 12.5 μl of 5× SDS sample buffer and boiled for 5 min. Proteins were resolved on polyacrylamide gels followed by immunoblotting with mouse anti-Flag (Sigma; 1:1000) and rabbit anti-Pangolin (1:700).

For the custom Pangolin antibody, a synthetic peptide ([H]-CK-Acp-MPHTHTRHGSSGDDL-[NH_2]) was used to immunize two rabbits (*8*) (Covance). The antiserum recognized three different isoforms of Pangolin in S2 cells (isoform J, 132 kD; isoforms B and H, 85 kD; isoform I, 49 kD), two of which specifically bound to Tcf binding sites.

Mad stability assay

To demonstrate stabilization of wild-type Mad by GSK3 inhibition, we transfected UAS–wild-type Mad-Flag or UAS–Mad-GM8 Flag with a metallothionein-Gal4 plasmid into S2R+ cells. Twelve hours after transfection, cells were treated with 100 mM $CuSO_4$ for 24 hours. Cells were then grown for a further 24 hours in the absence of $CuSO_4$, incubated with Wg medium for 12 hours, and lysed with radioimmunoprecipitation assay (RIPA) buffer. Western blots were performed using standard protocols. A rabbit α-Flag antibody (Sigma) was used to detect total amounts of wild-type Mad and Mad-GM8. A mouse α-Armadillo antibody was obtained from Developmental Studies Hybridoma Bank.

SUPPLEMENTARY MATERIALS

www.sciencesignaling.org/cgi/content/full/4/194/ra68/DC1

Fig. S1. Increased BMP signals generated by a stabilized Mad protein.
Fig. S2. Mad-GM8 expression increases the area of Distalless, a downstream target of Wg.
Fig. S3. Inducible RNAi directed against Wg depletes Wg protein and its downstream target Senseless.
Fig. S4. Mad-GM8 expression in the eye imaginal disc produces phenotypes suggestive of high Wg signaling.
Fig. S5. C-terminal phosphorylation of Mad enables BMP4 to repress the Mad-induced increase in Tcf reporter gene activity.
Fig. S6. The Mad RNAi phenotype is rescued by coexpression of a human Smad1 transgene.
Fig. S7. Mad is required for Wg signal transduction during wing margin development.
Fig. S8. Inhibition of GSK3 activity by BIO enhances the binding of Mad to Pangolin.
Table S1. Primer sequences.
References

REFERENCES AND NOTES

1. G. Schwank, K. Basler, Regulation of organ growth by morphogen gradients. *Cold Spring Harb. Perspect. Biol.* **2**, a001669 (2010).
2. C. Y. Logan, R. Nusse, The Wnt signaling pathway in development and disease. *Annu. Rev. Cell Dev. Biol.* **20**, 781–810 (2004).
3. N. T. Takaesu, D. S. Bulanin, A. N. Johnson, T. V. Orenic, S. J. Newfeld, A combinatorial enhancer recognized by Mad, TCF and Brinker first activates then represses *dpp* expression in the posterior spiracles of *Drosophila*. *Dev. Biol.* **313**, 829–843 (2008).
4. C. Estella, D. J. McKay, R. S. Mann, Molecular integration of wingless, decapentaplegic, and autoregulatory inputs into *Distalless* during *Drosophila* leg development. *Dev. Cell* **14**, 86–96 (2008).
5. H. Theisen, T. E. Haerry, M. B. O'Connor, J. L. Marsh, Developmental territories created by mutual antagonism between Wingless and Decapentaplegic. *Development* **122**, 3939–3948 (1996).
6. S. Morimura, L. Maves, Y. Chen, F. M. Hoffmann, *decapentaplegic* overexpression affects *Drosophila* wing and leg imaginal disc development and *wingless* expression. *Dev. Biol.* **177**, 136–151 (1996).

7. M. Domínguez, E. Hafen, Hedgehog directly controls initiation and propagation of retinal differentiation in the *Drosophila* eye. *Genes Dev.* **11**, 3254–3264 (1997).
8. L. C. Fuentealba, E. Eivers, A. Ikeda, C. Hurtado, H. Kuroda, E. M. Pera, E. M. De Robertis, Integrating patterning signals: Wnt/GSK3 regulates the duration of the BMP/Smad1 signal. *Cell* **131**, 980–993 (2007).
9. E. Eivers, L. C. Fuentealba, V. Sander, J. C. Clemens, L. Hartnett, E. M. De Robertis, Mad is required for Wingless signaling in wing development and segment patterning in *Drosophila*. *PLoS One* **4**, e6543 (2009).
10. M. Kretzschmar, J. Doody, J. Massagué, Opposing BMP and EGF signalling pathways converge on the TGF-β family mediator Smad1. *Nature* **389**, 618–622 (1997).
11. E. M. Pera, A. Ikeda, E. Eivers, E. M. De Robertis, Integration of IGF, FGF, and anti-BMP signals via Smad1 phosphorylation in neural induction. *Genes Dev.* **17**, 3023–3028 (2003).
12. C. Alarcón, A. I. Zaromytidou, Q. Xi, S. Gao, J. Yu, S. Fujisawa, A. Barlas, A. N. Miller, K. Manova-Todorova, M. J. Macias, G. Sapkota, D. Pan, J. Massagué, Nuclear CDKs drive Smad transcriptional activation and turnover in BMP and TGF-β pathways. *Cell* **139**, 757–769 (2009).
13. E. Aragón, N. Goerner, A. I. Zaromytidou, Q. Xi, A. Escobedo, J. Massagué, M. J. Macias, A Smad action turnover switch operated by WW domain readers of a phosphoserine code. *Genes Dev.* **25**, 1275–1288 (2011).
14. V. F. Taelman, R. Dobrowolski, J. L. Plouhinec, L. C. Fuentealba, P. P. Vorwald, I. Gumper, D. D. Sabatini, E. M. De Robertis, Wnt signaling requires sequestration of glycogen synthase kinase 3 inside multivesicular endosomes. *Cell* **143**, 1136–1148 (2010).
15. E. Eivers, L. C. Fuentealba, E. M. De Robertis, Integrating positional information at the level of Smad1/5/8. *Curr. Opin. Genet. Dev.* **18**, 304–310 (2008).
16. B. Müller, B. Hartmann, G. Pyrowolakis, M. Affolter, K. Basler, Conversion of an extracellular Dpp/BMP morphogen gradient into an inverse transcriptional gradient. *Cell* **113**, 221–233 (2003).
17. J. P. Couso, S. A. Bishop, A. Martinez Arias, The wingless signalling pathway and the patterning of the wing margin in *Drosophila*. *Development* **120**, 621–636 (1994).
18. H. A. Duong, C. W. Wang, Y. H. Sun, A. J. Courey, Transformation of eye to antenna by misexpression of a single gene. *Mech. Dev.* **125**, 130–141 (2008).
19. M. Schubiger, A. Sustar, G. Schubiger, Regeneration and transdetermination: The role of Wingless and its regulation. *Dev. Biol.* **347**, 315–324 (2010).
20. P. J. Bryant, Localized cell death caused by mutations in a *Drosophila* gene coding for a transforming growth factor-β homolog. *Dev. Biol.* **128**, 386–395 (1988).
21. P. Hoodless, T. Haerry, S. Abdollah, M. Stapleton, M. B. O'Connor, L. Attisano, J. L. Wrana, MADR1, a MAD-related protein that functions in BMP2 signaling pathways. *Cell* **85**, 489–500 (1996).
22. J. J. Sekelsky, S. J. Newfeld, L. A. Raftery, E. H. Chartoff, W. M. Gelbart, Genetic characterization and cloning of *Mothers against dpp*, a gene required for *decapentaplegic* function in *Drosophila melanogaster*. *Genetics* **139**, 1347–1358 (1995).
23. C. J. Neumann, S. M. Cohen, Long-range action of Wingless organizes the dorsal-ventral axis of the *Drosophila* wing. *Development* **124**, 871–880 (1997).
24. Y. A. Zeng, M. Rahnama, S. Wang, W. Lee, E. M. Verheyen, Inhibition of *Drosophila* Wg signaling involves competition between Mad and Armadillo/β-catenin for dTcf binding. *PLoS One* **3**, e3893 (2008).
25. J. Noordermeer, J. Klingensmith, N. Perrimon, R. Nusse, *dishevelled* and *armadillo* act in the Wingless signalling pathway in *Drosophila*. *Nature* **367**, 80–83 (1994).
26. M. Nishita, M. K. Hashimoto, S. Ogata, M. N. Laurent, N. Ueno, H. Shibuya, K. W. Cho, Interaction between Wnt and TGF-β signalling pathways during formation of Spemann's organizer. *Nature* **403**, 781–785 (2000).
27. E. Labbé, A. Letamendia, L. Attisano, Association of Smads with lymphoid enhancer binding factor 1/T cell-specific factor mediates cooperative signaling by the transforming growth factor-β and Wnt pathways. *Proc. Natl. Acad. Sci. U.S.A.* **97**, 8358–8363 (2000).
28. M. C. Hu, N. D. Rosenblum, Smad1, β-catenin and Tcf4 associate in a molecular complex with the Myc promoter in dysplastic renal tissue and cooperate to control Myc transcription. *Development* **132**, 215–225 (2005).
29. L. Meijer, A. L. Skaltsounis, P. Magiatis, P. Polychronopoulos, M. Knockaert, M. Leost, X. P. Ryan, C. A. Vonica, A. Brivanlou, R. Dajani, C. Crovace, C. Tarricone, A. Musacchio, S. M. Roe, L. Pearl, P. Greengard, GSK-3-selective inhibitors derived from Tyrian purple indirubins. *Chem. Biol.* **10**, 1255–1266 (2003).
30. S. Lei, A. Dubeykovskiy, A. Chakladar, L. Wojtukiewicz, T. C. Wang, The murine gastrin promoter is synergistically activated by transforming growth factor-β/Smad and Wnt signaling pathways. *J. Biol. Chem.* **279**, 42492–42502 (2004).
31. A. F. Candia, T. Watabe, S. H. Hawley, D. Onichtchouk, Y. Zhang, R. Derynck, C. Niehrs, K. W. Cho, Cellular interpretation of multiple TGF-β signals: Intracellular antagonism between activin/BVg1 and BMP-2/4 signaling mediated by Smads. *Development* **124**, 4467–4480 (1997).
32. R. Schwappacher, J. Weiske, E. Heining, V. Ezerski, B. Marom, Y. I. Henis, O. Huber, P. Knaus, Novel crosstalk to BMP signalling: cGMP-dependent kinase I modulates BMP receptor and Smad activity. *EMBO J.* **28** 1537–1550 (2009).
33. R. G. Wisotzkey, A. N. Johnson, N. T. Takaesu, S. J. Newfeld, α/β Hydrolase2, a predicted gene adjacent to *Mad* in *Drosophila melanogaster*, belongs to a new global multigene family and is associated with obesity. *J. Mol. Evol.* **56**, 351–361 (2003).
34. Y. S. Lee, R. W. Carthew, Making a better RNAi vector for *Drosophila*: Use of intron spacers. *Methods* **30**, 322–329 (2003).
35. D. M. Duncan, E. A. Burgess, I. Duncan, Control of distal antennal identity and tarsal development in *Drosophila* by *spineless–aristapedia*, a homolog of the mammalian dioxin receptor. *Genes Dev.* **12**, 1290–1303 (1998).
36. O. Korchynskyi, P. ten Dijke, Identification and functional characterization of distinct critically important bone morphogenetic protein-specific response elements in the Id1 promoter. *J. Biol. Chem.* **277**, 4883–4891 (2002).
37. H. Inoue, T. Imamura, Y. Ishidou, M. Takase, Y. Udagawa, Y. Oka, K. Tsuneizumi, T. Tabata, K. Miyazono, M. Kawabata, Interplay of signal mediators of decapentaplegic (Dpp): Molecular characterization of mothers against dpp, Medea, and daughters against dpp. *Mol. Biol. Cell* **9**, 2145–2156 (1998).
38. M. T. Veeman, D. C. Slusarski, A. Kaykas, S. H. Louie, R. T. Moon, Zebrafish prickle, a modulator of noncanonical Wnt/Fz signaling, regulates gastrulation movements. *Curr. Biol.* **13**, 680–685 (2003).
39. J. C. Clemens, C. A. Worby, N. Simonson-Leff, M. Muda, T. Maehama, B. A. Hemmings, J. E. Dixon, Use of double-stranded RNA interference in *Drosophila* cell lines to dissect signal transduction pathways. *Proc. Natl. Acad. Sci. U.S.A.* **97**, 6499–6503 (2000).
40. U. Persson, H. Izumi, S. Souchelnytskyi, S. Itoh, S. Grimsby, U. Engström, C. H. Heldin, K. Funa, P. ten Dijke, The L45 loop in type I receptors for TGF-β family members is a critical determinant in specifying Smad isoform activation. *FEBS Lett.* **434**, 83–87 (1998).

41. **Acknowledgments:** We thank E. Verheyen, I. Duncan, H. Bellen, M. Affolter, S. Newfeld, M. O'Connor, N. Baker, C. Heldin, R. Nusse, and R. Moon, Developmental Studies Hybridoma Bank, Bloomington Stock Center, and the Vienna *Drosophila* RNAi Center for reagents; R. Dobrowolski and D. Ploper for comments on the manuscript; and K. Ngo for help with statistical analysis. We thank J. Olsen and U. Banerjee for the use of their scanning electron microscope. **Funding:** This work was supported by the NIH (HD21502-25) and the Howard Hughes Medical Institute, of which E.M.D.R. is an investigator. **Author contributions:** Experiments were performed by E.E. and H.D. (Figs. 1 to 4) with assistance from R.H.C. (parts of Fig. 1). E.E., H.D., and E.M.D.R. contributed to the experimental design and writing of the manuscript. **Competing interests:** The authors declare that they have no competing interests.

Submitted 23 March 2011
Accepted 19 September 2011
Final Publication 11 October 2011
10.1126/scisignal.2002034
Citation: E. Eivers, H. Demagny, R. H. Choi, E. M. De Robertis, Phosphorylation of Mad controls competition between Wingless and BMP signaling. *Sci. Signal.* **4**, ra68 (2011).

Science Signaling
AAAS
www.sciencesignaling.org/cgi/content/full/4/194/ra68/DC1

Supplementary Materials for

Phosphorylation of Mad Controls Competition Between Wingless and BMP Signaling

Edward Eivers, Hadrien Demagny, Renee H. Choi, Edward M. De Robertis*

*To whom correspondence should be addressed. E-mail: ederobertis@mednet.ucla.edu

Published 11 October 2011, *Sci. Signal.* **4**, ra68 (2011)
DOI: 10.1126/scisignal.2002034

The PDF file includes:

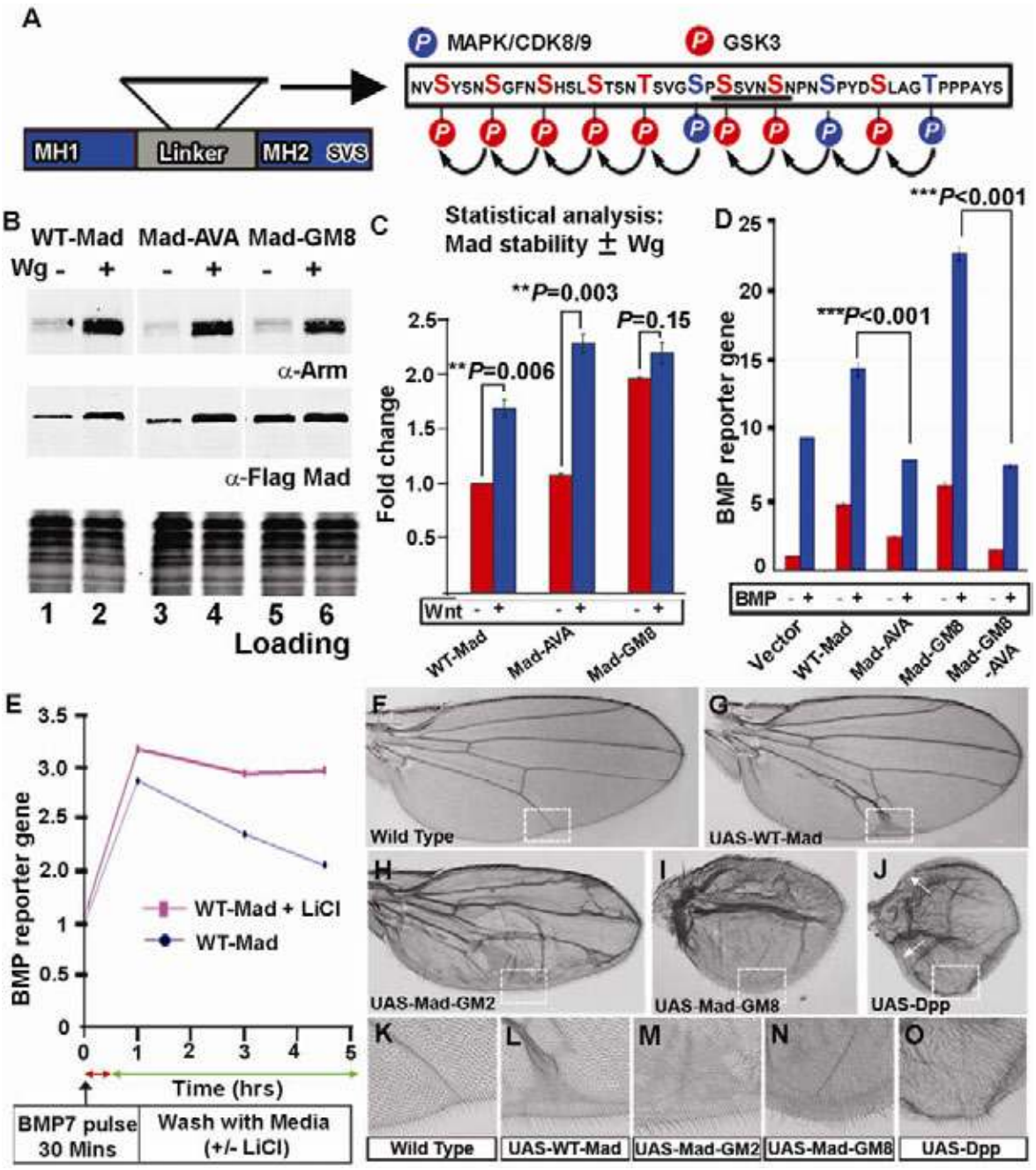

figure S1. Increased BMP signals generated by a stabilized Mad protein. In the Mad GSK3 mutant 8 (Mad-GM8), the eight putative GSK3 sites were rendered resistant to phosphorylation by mutating Ser or Thr to Ala. **(A)** Schematic diagram highlighting the putative phosphorylation sites in the linker region of Mad. Three potential MAPK or CDK8 and CDK9 priming phosphorylations (Ser-Pro) are highlighted in blue. The eight putative GSK3 phosphorylations in

Mad are indicated in red. **(B)** Flag-tagged WT-Mad is significantly stabilized in cells treated with Wg-conditioned medium compared to cells treated with conditioned medium from cells not transfected with Wg (compare lanes 1 and 2). Mad-AVA, which is resistant to C-terminal phosphorylation, is also stabilized by Wg protein (lanes 3 and 4). Mutation of all eight GSK3 phosphorylation sites in the linker region of Mad (Mad-GM8) causes stabilization of the protein even in the absence of Wg conditioned medium (lanes 5 and 6). Armadillo, a protein that is stabilized by Wg, is used to demonstrate activation of Wg signaling. Equal loading is shown in the coomassie blue image (n = 4 blots). **(C)** Analysis by Mann-Whitney-Wilcoxon test of the stability of Mad from immunoblots quantified using the LI-COR Odyssey system. **(D)** BMP reporter gene (BRE-luciferase) activity was increased when GSK3 phosphorylation sites in Mad (Mad-GM8) were mutated. BMP stimulation did not increase BMP reporter activity above basal values in cells expressing Mad-GM8-AVA ($P < 0.001$, brackets; 2-way ANOVA with Tukey's post-test). These experiments demonstrate that Mad-GM8 enhances the effects of BMP signaling by increasing the duration of the BMP signal, but only when C-terminal phosphorylation is possible (n = 3 experiments). **(E)** 30-minute incubation with BMP7 was performed at the beginning of this assay. The duration of the BMP signal was prolonged by inhibiting GSK3 phosphorylation with LiCl, a treatment that mimics the Wg signal. **(F)** Wild-type adult wing, showing normal venation. **(G)** A moderate increase in vein tissue in adult wings was seen when WT-Mad was driven with MS1096-Gal4 (n = 23). **(H)** In adult wings with a form of Mad bearing two mutated GSK3 phosphorylation sites (Mad GSK3 mutant 2; Mad-GM2), vein formation was increased (n = 34) (*1*). **(I)** Overexpression of Mad-GM8 protein resulted in increased venation (n = 45, all specimens showed similar phenotypes). The shape of the adult wing also adopted a more circular shape compared to wild-type wings. **(J)** Dpp overexpression generated vein and wing shape phenotypes similar to those of Mad-GM8 overexpression (n =

20). Dpp overexpression causes loss of margin bristles (white arrows), a typical Wg loss-of-function phenotype (*2*). **(K)** High magnification of boxed region in (B) showing the distal portion of vein 5. Note that vein cells were smaller than intervein cells. **(L)** High magnification of longitudinal vein 5 showing that WT-Mad overexpression mildly increased distal venation forming a delta structure towards the margin. **(M)** High magnification of Mad-GM2 overexpressing wings showing transformation of intervein tissue into vein tissue. **(N)** High magnification of Mad-GM8 overexpressing wings showing that intervein tissue displayed the smaller cell phenotype characteristic of vein tissue. **(O)** Dpp overexpression, like Mad-GM8 overexpression, transforms intervein tissue into vein tissue.

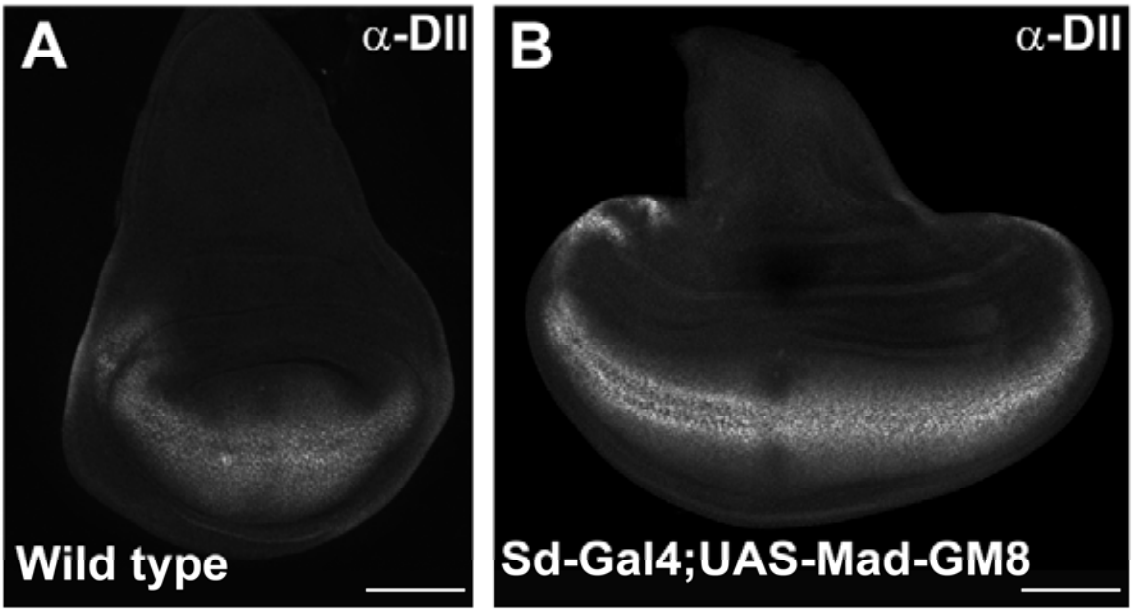

figure S2. Mad-GM8 expression increases the area of Distalless, a downstream target of Wg. **(A)** Distribution of Distalless in a wild-type wing imaginal disc at 3rd instar larval stage (n = 24 discs). Distalless is strongest along the presumptive wing margin and weaker in other regions of the wing pouch (n = 14 discs). **(B)** Overexpression of Mad-GM8 using Scalloped-Gal4 wing disc increases the area of Distalless in the wing pouch (n = 15). The shape of the wing disc is also extended along the anterior-posterior axis, and the overall size increased, as is typical of wing discs with increased Dpp signaling (*3*). Scale bars, 100 µm.

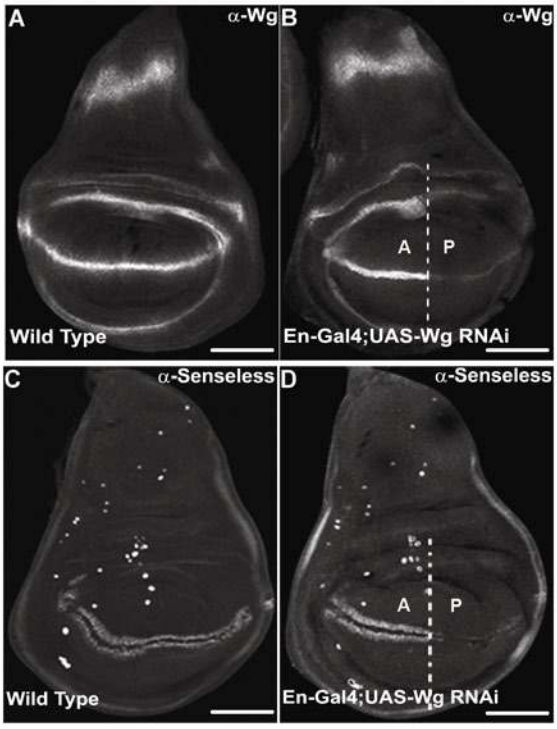

figure S3. Inducible RNAi directed against Wg depletes Wg protein and its downstream target Senseless. **(A)** Wild-type distribution of Wg protein in 3rd instar larval wings imaginal discs (n = 20 discs). **(B)** Wg RNAi in the posterior (P) wing compartment driven by *Engrailed-Gal4* reduced Wg protein abundance (n = 18). **(C)** Wild-type distribution of Senseless, a downstream target of Wg target (n = 40 discs). **(D)** Senseless is lost in the posterior wing compartment when Wg is knocked down by RNAi driven by *Engrailed*-Gal4 (n = 23 discs). These results demonstrate that the Wg RNAi construct used (VDRC #13352) is effective in *Drosophila*. Scale bars, 100 µm.

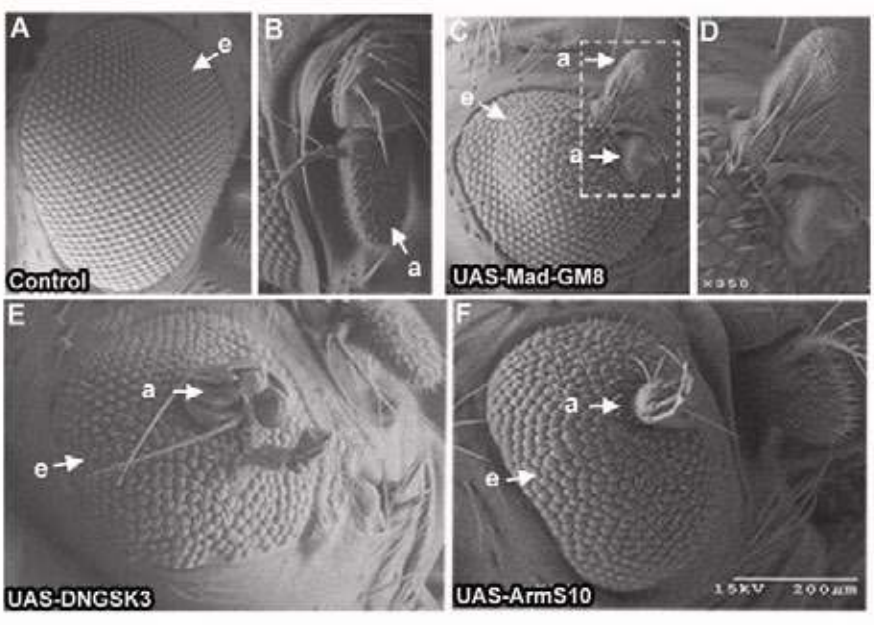

figure S4. Mad-GM8 expression in the eye imaginal disc produces phenotypes suggestive of high Wg signaling. **(A)** Image of wild-type adult eye (e) and **(B)** antenna (a) by scanning electron microscopy. **(C)** Transformation of part of the *Drosophila* eye into antennal-like tissue when Mad-GM8 was driven by *eyeless-Gal4* (n = 66 eyes with ectopic antennae or bulging structures out of 97 eyes). **(D)** A high power image of two ectopic antennal-like growths induced by Mad-GM8 overexpression. **(E)** Similar antennal-like structures were observed when Wg signaling was activated by dominant negative GSK3 (DNGSK3) (n = 24 eyes) or **(F)** stabilized Armadillo (ArmS10) driven by *eyeless-Gal4* (n = 13 eyes). This experiment shows that overexpression of the stabilized, GSK3 phosphorylation-resistant form of Mad elicits a canonical Wg signal.

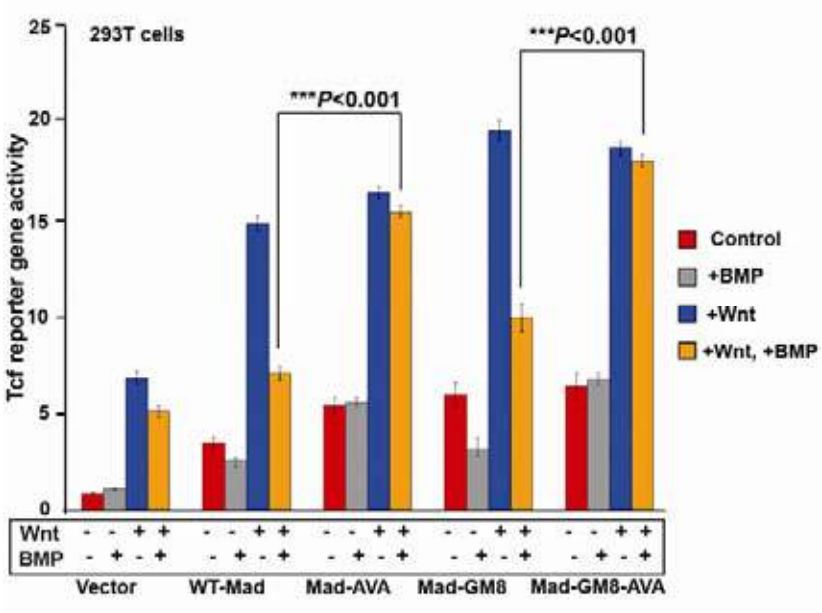

figure S5. C-terminal phosphorylation of Mad enables BMP4 to repress the Mad-induced increase in Tcf reporter gene activity. Mad forms resistant to phosphorylation by BMP receptor are insensitive to inhibition of Wnt signaling by BMP4. W-Mad or Mad mutant proteins (Mad-AVA, Mad-GM8, or Mad-GM8-AVA) increased Wnt reporter activity compared to control cells. A comparable increase in Wnt activity was found when cells were transfected with WT-Mad or Mad-AVA (the C-terminal phosphorylation mutant), an effect that can be attributed to the lack of endogenous BMP signaling in HEK293T cells. In the case of *Drosophila* S2R+ cells, which have endogenous BMP signaling, Mad-AVA stimulated the activity Tcf reporter (Fig. 2B). Expression of a form of Mad with mutations in the 8 putative GSK3 phosphorylation sites in the linker region increased Wnt reporter activity compared to WT-Mad. Also, BMP4 treatment of cells failed to induce significant Tcf reporter activation (grey bars). Treating cells with both Wnt and BMP4 inhibited the ability of WT-Mad to increase Wnt-reporter activity, but not in cells expressing C-terminal mutant forms of Mad (Mad-AVA and Mad-GM8-AVA; see brackets). We propose that phosphorylation of Mad by BMP receptor prevents Mad from signaling in the Wnt pathway (n = 3 experiments; statistical analysis was carried out with a 2-way ANOVA with

Tukey’s post-test).

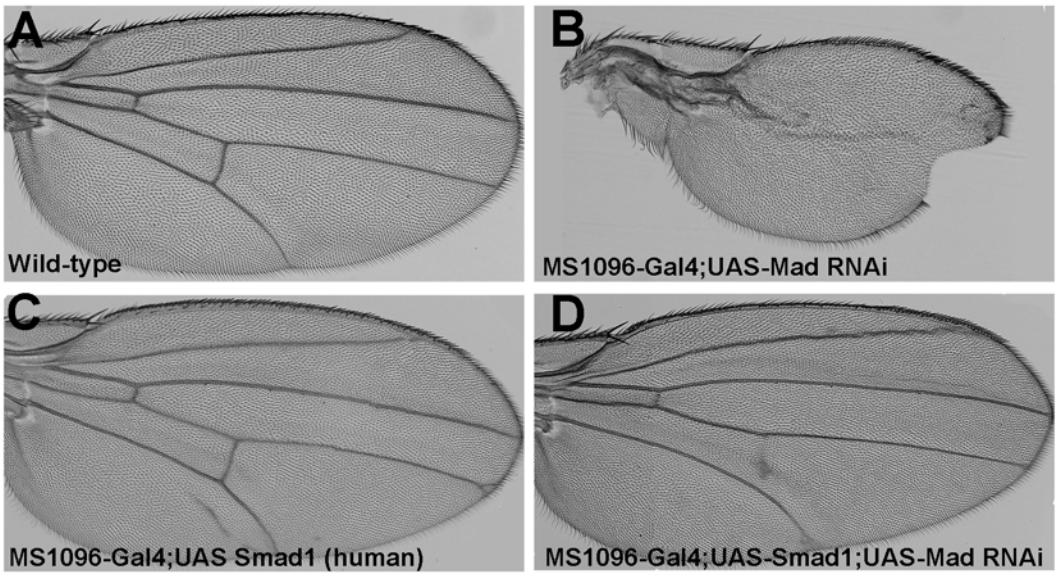

figure S6. The Mad RNAi phenotype is rescued by coexpression of a human Smad1 transgene. **(A)** Wild-type adult wing, showing normal venation, which requires BMP signaling (n = 30 wings). **(B)** Loss of vein tissue and margin notching in Mad-RNAi adult wings (n = 25). **(C)** Overexpression of a UAS-Smad1 human produced some extra vein tissue, but the wing was largely normal (n=15). **(D)** The Mad RNAi phenotype was rescued (except for the posterior crossvein) when a human Smad1 transgene was expressed (n=9).

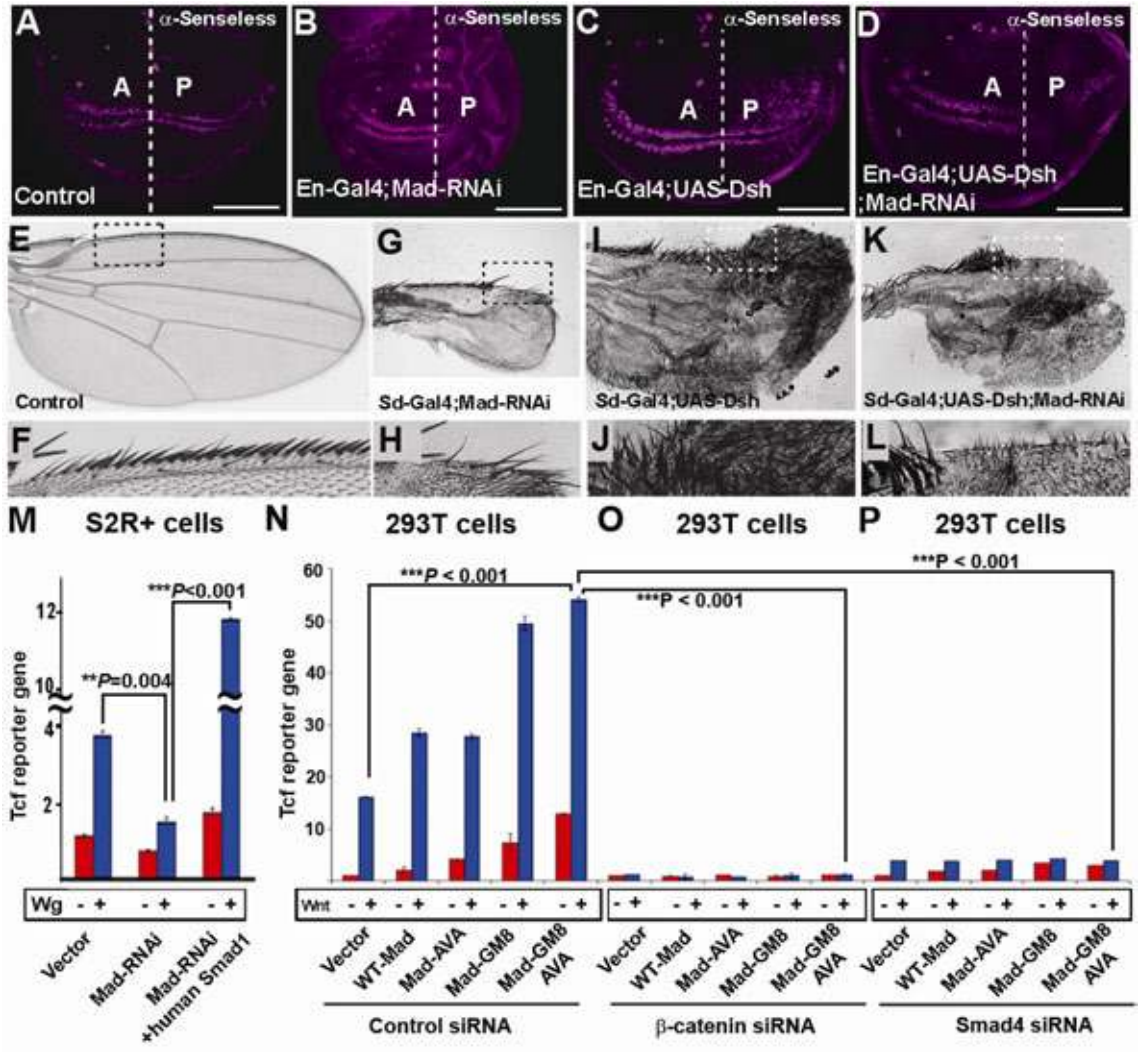

figure S7. Mad is required for Wg signal transduction during wing margin development. **(A)** Distribution of Senseless in 3rd instar wild-type wing imaginal disc. Anterior-posterior axis of the wing disc is indicated as A and P. **(B)** Mad knockdown using an RNAi driven by Engrailed-Gal4 specifically in the posterior wing compartment reduces the area of Senseless. **(C)** Overexpression of Dishevelled in the posterior compartment causes ectopic areas of Senseless. **(D)** Ectopic Senseless is blocked by Mad-RNAi expression in the posterior compartment. Mad RNAi is epistatic to Dishevelled, indicating that Mad is required downstream of Dishevelled in the Wnt pathway. At least 12 imaginal discs were analyzed for each genotype, all with similar

phenotypes. **(E)** Wild-type adult wing. **(F)** High magnification of the anterior wing margin (highlighted as a boxed region in E). **(G** and **H)** Mad RNAi driven with Scalloped-Gal4 results in a small veinless wing. This wing is deficient in margin bristles, which suggests loss of Wg signaling (n = 45 wings). **(I** and **J)** Overexpression of Dishevelled caused increased bristle formation throughout the wing blade (n = 38 wings). **(K** and **L)** Increased bristle formation in the wing blade caused by Dishevelled was inhibited when Mad was knocked down using RNAi (n = 24). **(M)** Mad knockdown by Gal4-inducible RNAi inhibited Tcf reporter gene activation, which was rescued by transfection of human WT-Smad (n = 5 experiments, statistical analysis carried out using a 2-way ANOVA with Tukey's post-test). **(N** to **P)** Activation of the Tcf reporter gene by Mad constructs in the presence of control siRNA, β-catenin siRNA, or Smad4 siRNA in HEK293T cells. Treating cells with a control siRNA had no effect on Tcf reporter gene activation. siRNA-mediated depletion of β-catenin blocked activation of the canonical Wnt pathway. Treatment of cells with Smad4 siRNA also efficiently blocked Wnt signaling. This shows that both Smad4 and β-catenin are essential components of the Wnt signaling pathway (n = 3 experiments, statistical analysis carried out using a 2-way ANOVA with Tukey's post-test). Scale bars 100 μm.

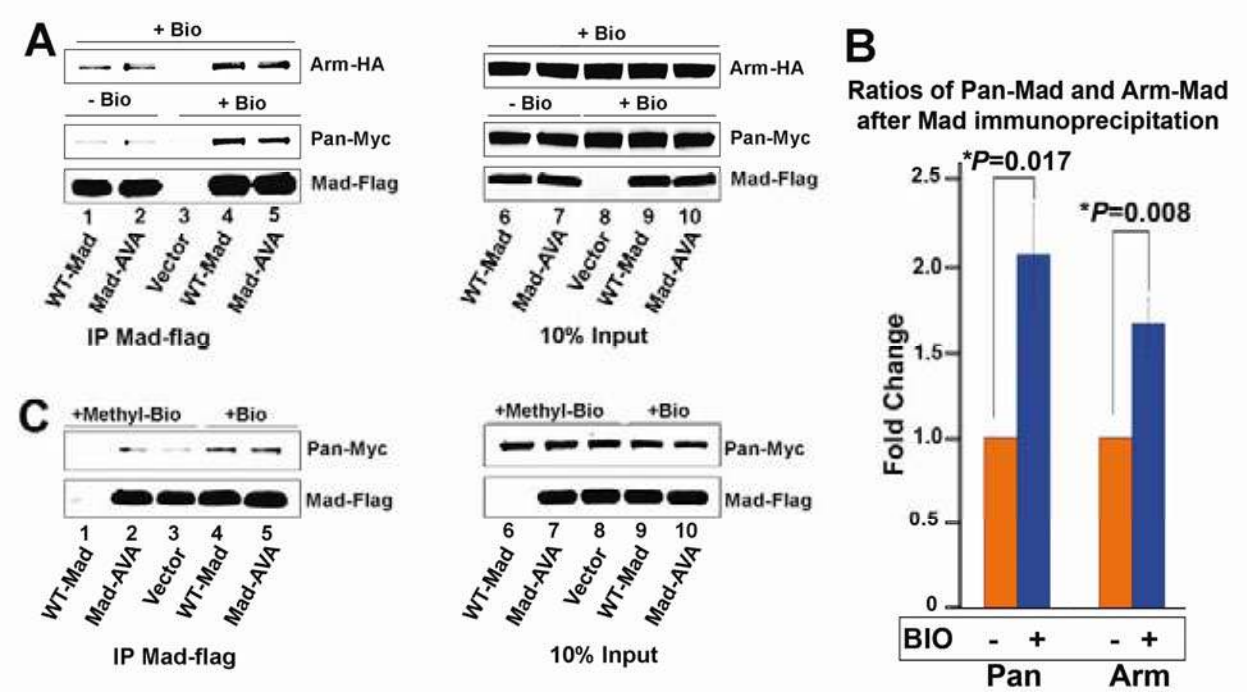

figure S8. Inhibition of GSK3 activity by BIO enhances the binding of Mad to Pangolin. **(A)** Coimmunoprecipitation of Pangolin-Myc and Armadillo-HA through Mad-Flag or Mad-AVA-Flag (lanes 1-5). Pangolin and Mad DNAs were transfected separately into HEK293T cells and treated with or without the GSK3 inhibitor BIO. Cells expressing Armadillo were subjected to BIO treatment under all conditions to ensure sufficient protein amounts. Input proteins (lanes 6-10) shown are 10% of the amount used for the binding experiments. Cell lysates containing Mad proteins were incubated with separate lysates containing Pangolin and Armadillo proteins for one hour at 4^{o}C to allow binding. In the absence of BIO, we observed only weak binding between Mad and Pangolin (lanes 1 and 2, minus BIO). Treating HEK293T transfected cells with BIO enhanced the binding of Mad to Pangolin (lanes 4 and 5, +BIO), indicating that the phosphorylation of Mad by GSK3 inhibits binding between Mad and Pangolin. Based on these findings, we propose that Wnt signaling promotes the binding of Mad to Pangolin by preventing GSK3 phosphorylations, in addition to stabilizing Armadillo (n = 3 experiments). **(B)** Quantification of the ratio of immunoprecipitated Pangolin and Armadillo protein over Mad

using a LI-COR Odyssey scanner system. Treatment with the GSK3 inhibitor BIO caused a 2-fold increase in binding efficiency between Mad and Pangolin and a 1.5 -fold increase in binding efficiency to Armadillo in HEK293T cell extracts (P = 0.0017, P = 0.008, Mann-Whitney Wilcoxon test, n = 3). **(C)** We also used an inactive form of this compound, methylated-BIO, to test whether BIO had non-specific off target effects. In cells treated with methylated-BIO, there was less binding of Mad to Pangolin (lanes 2 and 3) when compared to the active form of BIO (lanes 4 and 5).

Table S1. Primer Sequences: Primers used for the double stranded RNAi experiments and the Biotin labeled primers used to PCR the 7x TOPFLASH or FOPFLASH Pangolin binding sites for DNA Affinity Precipitation Assay (DAPA)

Primer name	Sequence
dsRNA Mad 5’	TTAATACGACTCACTATAGGGAGAGTCATGGTCACACTGTTTTCAATGG
dsRNA Mad 3’	TTAATACGACTCACTATAGGGAGACTGTTGCTGCTGCCGCTGATTGCTG
dsRNA Med 5’	TTAATACGACTCACTATAGGGAAGTGCGTGACCATACAGCGCACC
dsRNA Med 3’	TTAATACGACTCACTATAGGGATTCAGAGGGACCCTGTGGATATCCG
dsRNA Arm 5’	GGATTAATACGACTCACTATAGGGAGACAACTGAGCCAGACACGC
dsRNA Arm 3’	GGATTAATACGACTCACTATAGGGAGAGCTCTCCTGGTTACCATAGG
DAPA primer 5’	Biotin-CAGGTGCCAGAACATTTCTC
DAPA primer 3’	AAGCTGGAATTCGAGCTTCC

References

1. E. Eivers, L.C. Fuentealba, V. Sander, J.C. Clemens, L. Hartnett, E.M. DeRobertis, Mad is required for Wingless signaling and segment patterning in Drosophila and Xenopus. *PLoS One* **4**, e6543 (2009).
2. J. P. Couso, S. A. Bishop, A. Martinez-Arias, The wingless signalling pathway and the patterning of the wing margin in Drosophila. *Development* **120**, 621-636 (1994).
3. T. Lecuit, W.J. Brook, M. Ng, M. Calleja, H. Sun, S.M. Cohen. Two distinct mechanisms for long-range patterning by Decapentaplegic in the Drosophila wing. *Nature* **381**, 387-393 (1996).